IPTC 17447

Estimation of Rock Compressive Strength Using Downhole Weight-on-Bit and Drilling Models

Prasad B. Kerkar, Shell International E&P Inc.; Geir Hareland, Oklahoma State University; Ernesto R. Fonseca and Claudia J. Hackbarth, Shell International E&P Inc

This paper was prepared for presentation at the International Petroleum Technology Conference held in Doha, Qatar, 20–22 January 2014.

Abstract

In unconventional gas and tight oil plays, knowledge of the in situ rock mechanical profiles of the reservoir interval is critical in planning horizontal well trajectories and landing zones, placement of perforation clusters along the lateral, and optimal hydraulic fracture stimulation design. In current practice, vertical pilot holes and/or the laterals are logged after drilling, and the sonic and neutron log results are interpreted along with mechanical rock properties measured in the laboratory on core material. However, coring, logging, and core analyses are expensive and time consuming. In addition, as they are typically only performed in a few wells that are assumed to be representative, there is considerable uncertainty in extrapolating results across wide areas with known variability in stratigraphy, faults, thicknesses, hydrocarbon saturations, etc.

This paper reports a method for estimating mechanical rock properties and in situ rock mechanical profiles in every well in a development, based on calibration from initial rock core analyses plus drilling data that is routinely acquired. Wellbore friction analysis was coupled with a torque and drag model to estimate in situ unconfined compressive strength (UCS) and Young's modulus (YM) profiles. The key process steps include: a) Calculate the weight and wellbore friction force of each element of the drill string from bottom to the surface; b) Adjust the hook load (HL) by subtracting the weight of the hook and entire drill string; c) Iteratively compute the friction coefficient to match calculated and observed HL; d) Estimate downhole weight-on-bit (DWOB) by applying a stand pipe pressure correction to the calculated HL and considering potential sliding and abrasiveness; e) Use a rate of penetration (ROP) model developed for polycrystalline diamond compact (PDC) drill bits considering a force balance between a drill bit geometry and formation and a wear function depending upon the formation abrasiveness and bit hydraulics to compute confined compressive strength (CCS). The resulting CCS was correlated to UCS and YM using regression constants obtained from laboratory triaxial test data on whole core. Using examples from horizontal wells in a siltstone play in Alberta, Canada, this manuscript demonstrates a workflow to estimate rock strength from drilling data. The predicted UCS and YM values were compared with log data and potential uncertainties arising out of drilling data are discussed.

Introduction

In conventional and unconventional plays alike, a typical way to characterize the subsurface is to make measurements of the formation penetrated by the wellbore with logging tools that are either carried behind the drill bit (logging while drilling) or else run in the well after the drill string is removed (wireline or drill pipe-conveyed logging). Because this adds cost and risk, for unconventional gas or tight oil (UGTO) projects that may have hundreds to even thousands of producers, typically only early appraisal wells plus later, areally scattered wells are designed with extensive logging and laboratory core characterization programs. The assumption is that lateral variability and local heterogeneties are not great and that these data-rich penetrations sufficiently constrain the reservoir properties in the areas between them. In UGTO projects, good representations of the in situ stress profile and geomechanical rock properties are required to optimize the well trajectories and landing zones, placement of perforation clusters along the lateral, and hydraulic fracture stimulation design.

Drilling operations have advanced with real-time monitoring, control, automation, data acquisition and data mining

(Rassenfoss, S., 2011). Such real-time data could be effectively used to understand downhole dynamics and formation characteristics. Real-time wellbore fluid dynamics and wellbore friction factors were shown to identify hole cleaning efficiency, stuck pipe, differential sticking, formation changes and mud lubrication issues (Falconer et al., 1989). Measurements of DWOB, downhole torque and surface weight-on-bit (SWOB) were demonstrated to be effective in assessing and optimizing the performance of a bit, mud motor and bottomhole assembly while drilling through sand/shale sequences or formations which are difficult to steer through (Belaskie et al., 1993). This approach was shown to reduce trial and error based approach, excessive drill bit wear, unnecessary trips and rig time. Eshkalak et al. (2013) demonstrated generating geomechanical logs from conventional logs (Gamma Ray, Density and Porosity) using artificial intelligence. Building on this foundation, valuable reservoir characteristics obtained from logging/coring programs from the pilot wells can be coupled with measurements while drilling. Drilling data signatures such as HL, ROP, drill bit revolutions per minute (RPM), well trajectory and drilling fluid dynamics may be utilized to understand geomechanical properties of formation and their variations from every well. Several previous studies were performed to develop ROP models based on drill bit specification, wellbore friction and DWOB calculations and combine ROP, wellbore friction and DWOB to calculate rock properties such CCS, UCS and YM. The following sections review previous work on drill bit models, wellbore friction, DWOB and ROP inversion to predict rock strength.

Drill bit models

Warren (1984) established a relationship between weight-on-bit (WOB) and the depth of tooth penetration for a roller cone bit. Burgess and Lesso (1985) evaluated a new versus a couple of worn milled-tooth roller cone bits on Pierre shale at constant mud flow rate, borehole pressure and isotropic stress conditions. The new drill bit followed a straight line correlation when the dimensionless torque was plotted against the dimensionless penetration rate defined as ROP/ (RPM.D_b). The intercept and slope values of the plots were found to be consistent with those for a similar new drill bit tested in shale and sand sequence in the Gulf Coast of the USA. The worn out bits deviated from the straight line correlation due to the lower torque. Winters et al. (1987) presented a bit model that related rock CCS and ductility. The bit design constants computed after regressing laboratory drilling data are applicable for all styles of roller cone bit designs. Kuru and Wojtanowsicz (1988) derived a drilling model based on force balance at the PDC bit cutter and formation which combined the torque, drilling rate, cutter geometry and formation characteristics. A plot of dimensionless torque against dimensionless drilling rate was suggested as a diagnostic tool from early drilling where a new bit data followed a straight line and subsequent data showed scatter depending upon the bit wear.

Wellbore friction and DWOB

A large part of energy from the kelly/top-drive is spent to overcome friction during drilling. Several investigations were performed to estimate friction factors along the wellbore and DWOB. Lesage et al. (1988) used equations (Johancsik et al. 1984) that relate DWOB, SWOB and torque to estimate the wellbore friction factor for two field cases where both downhole and surface torque and WOB sensors were utilized. Most of the values of the friction factor ranged between 0.25 and 0.4, lost circulation in permeable zones probably due to reduced buoyancy and excessive WOB. Falconer et al. (1989) used real-time measurements of DWOB, SWOB and torque to compute rotating and sliding friction factors while drilling for 6 case studies which emphasized the use of friction factor in diagnosing drilling problems. The parameters such as filter cake thickness, differential sticking, and build up of cuttings in the annulus gradually increase wellbore friction, whereas hanging stabilizers contribute in sharp increase in frictional forces. In the cases presented, friction factor during normal rotary drilling ranged between 0.18 and 0.22 and was observed to be relatively constant in the partially cased hole. Unsworth et al. (1990) introduced a method for accurate depth measurement which comprised of automated pipe tally listings, ROP, drill string tension based slipping criterion and continuous monitoring of the drill bit while tripping. Belaskie et al. (1993) measured DWOB and torque while slanted/horizontal drilling through shale, interbedded sand-shale and the Sadlerochit formations in Lisburne field on the North Slope of Alaska. The knowledge of real-time DWOB/SWOB and torque was found to be effective in understanding undergauged/locked cone bit, fractured motor shaft and packed-hole assembly problems and hence performing only necessary trips. The values of dimensionless torque (T_D) defined as $T_D = 12T_{dh}$[ft-klbs] /[DWOB.D_b] were found to be ~0.3 for shales. Luke and Juvkam-Wold (1993) derived equations for HL as a function of derrick load, dead-line tension, individual sheave efficiency and number of lines between blocks for the active and inactive dead-line sheaves while raising and lowering traveling block. Such HL dependence was verified with a block-and-tackle system involving a workover rig, crown block, traveling block and load acquisition devices. Reiber et al. (1999) calculated incremental and total wellbore friction factors with bottom-up drill string weight calculations performed on real-time well data and from offshore Norway, Denmark, and onshore Germany. The changes in friction factors were utilized in identifying stuck pipe/differential sticking, mud lubricity, hole cleaning, formation changes and effectiveness of torque reduction tools. Aadnoy and Andersen (2001) established analytical solutions to predict wellbore friction for different well geometries in vertical and horizontal planes with survey parameters such as inclination and azimuth. These solutions were further formulated in 3-dimensions and applied to a deviated well with additional parameters such as dogleg and dogleg severity (Aadnoy et al., 2010; Fazaelizadeh et al, 2011).

ROP models for rock strength

Rampersad et al. (1993) used ROP models derived for roller cone and PDC bits by Warren (1984) and Kuru and Wojtanowsicz (1988) respectively, to compute drill bit and wear coefficients at optimum ROP. Such optimum ROP values were utilized to predict CCS and UCS to create a geological-drilling-log (GDL) for each drill bit and corresponding intervals. Hareland and Hoberock (1993) later introduced a wellbore cleaning efficiency function and applied it to ROP models of tricone rollercone drill bit performance to generate CCS and UCS profiles from drilling data of 3 wells in East Texas and one well from southwestern Wyoming drilled in Catoosa shale and Carthage limestone lithologies respectively for which good agreement was observed with field closure test data. Hareland et al. (1996) further developed a drill bit wear factor as a function of abrasiveness of a rock. These ROP models along with lithology coefficients obtained from laboratory data were utilized to predict CCS profiles in a Norwegian field drilled with a combination of PDC and rollercone bit (Hareland and Nygaard, 2007). A correlation between CCS and UCS was presented to account for both overbalanced and underbalanced drilling (Shirkavand et al., 2009). Hareland et al. (2010) observed indentation of a rollercone with a single row of inserts on different rock samples to develop a rock failure model for rollercone bits which predicted UCS trends consistent with those predicted from logs.

Case Study and Methodology

The extension of these concepts to unconventional gas/ tight oil plays requires further adaptation. Shale formations typically cover larger areas, exhibit natural fractures, may have drilling hazards and vary in hydrocarbon and water saturation. Drilling fluid characteristics, wellbore trajectory and drilling, completion and stimulation designs need to be tailored for optimal performance. Ajayi et al. (2013) reported that perforation clusters or fracture stages located in wellbore intervals of relatively low minimum principal stress or similar geomechanical properties resulted in 33-40% higher gas flowback rates from two wells drilled in Marcellus Shale reservoirs in Pennsylvania and New York, USA. Therefore characterizing geomechanical properties such as UCS and YM while drilling could be related to rock brittleness which would provide significant advantage in designing stimulations with optimized stage-spacing, fracture length and orientation.

In this study, drilling data were utilized to predict UCS and YM in horizontal section of a wellbore. Horizontal wells drilled and completed in the Lower Triassic Montney Formation E lobe, Alberta, Canada were analyzed for rock strength prediction from drilling data. The well (Well A) orientation and geological layers encountered while drilling are shown in Figure 1. The Montney typically consists of dark grey siltstone with minor sandstone to dolomitic siltstone. It exhibits 131-170^{o}F in situ temperature, 2-4.5 wt% total organic carbon and 3-10% porosity with 30-70% gas saturation (Nieta et al., 2009; Walsh et al., 2006). The Montney Formation is overlain by the middle Triassic Doig Formation (~150 m) which includes granular phosphate and phosphatic pebbles (Edwards et al., 2012). Drilling parameters collated under survey-, depth- and time-based data are listed in Figure 2. Depth- and time-based drilling data were acquired from the well's drilling database. The depth-based data used was every 0.5 m whereas time-based data was every 20 seconds. Additional parameters such as pore pressure, mud weight, plastic viscosity and mud type (oil/water-based) were compiled from daily drilling reports (Table 1). Pore pressure was obtained from a post-drilling diagnostic fracture injection test (DFIT) as 14.58 kPa/m (2.11 psi/m; specific gravity: 1.49) which confirmed underbalanced drilling conditions in the lateral section of the wellbore. Drill string specifications (Table 2) such as number of joints, length of each joint, outer diameter, inner diameter and unit mass were obtained from a daily drilling reports at the bottom section of zone of interest (measured depth: 4490m). The horizontal section of the well (total depth: 2600-4490 m) was drilled with a PDC drill bit (MSF513M) manufactured by ReedHycalog. Specifications of the drill bit (Table 3) were obtained from drill bit summary available in the drilling database. Drilling rig parameters such as weight of the hook, number of lines and sheave efficiency were assumed as 12 kDaN (27 klbs), 10 and 98% respectively.

The depth- and time-based data were filtered to eliminate erroneous data points (e.g. RPM, and ROP < 0) due to uncertainties while drilling, tripping and non-productive time. No other drilling parameter was adjusted to avoid errors due to individual bias. Figure 3 shows SWOB, HL, ROP and top-drive RPM from the depth-based file. The measured HL was adjusted for frictional losses in the sheaves of the hoisting system (Eq. 1-2) after subtracting the weight of the hook (Dangerfield, 1987).

$$SheaveHL = \frac{HL_{obs}}{n_{lines}} \cdot \frac{e\left(1 - \frac{1}{e^{n_{lines}}}\right)}{e-1} \quad \text{(raising block)} \tag{1}$$

$$SheaveHL = \frac{HL_{obs}}{n_{lines}} \cdot \frac{1 - e^{n_{lines}}}{1-e} \quad \text{(lowering block)} \tag{2}$$

The resultant value of the HL was further corrected by subtracting the product of differential pressure and cross-sectional area of the drill pipe. This correction accounts for the stretch of the drill string. Using drill string specifications, the weight of each element of the drill string was calculated from the drill string weight of that element times the buoyancy factor. Survey data was utilized to determine if the element was in tension or compression to use the appropriate force equation. These forces were added up from bottom to the surface (Fazaelizadeh, et al., 2011) to compute net HL. Time-based data were used to identify off-bottom (bit depth = total depth) calibration depths at which friction factors were determined iteratively to match surface HL and net HL within 0.5 kDaN tolerance using equation 3 or 4 (Dashevskiy et al., 2006). DWOB was subsequently adjusted by applying stand pipe pressure correction to the calculated HL. DWOB values could be further subjected to potential sliding criterion (Eq. 5) in build-up section of the wellbore and abrasiveness constants for different formations (Table 4).

$$F_{top} = \beta w \Delta L\left(\cos\alpha \quad or \quad \frac{\sin\alpha_{top} - \sin\alpha_{bottom}}{\alpha_{top} - \alpha_{bottom}}\right) - \mu \times \beta w \Delta L\left(\sin\alpha \quad or \quad \frac{\cos\alpha_{top} - \cos\alpha_{bottom}}{\alpha_{top} - \alpha_{bottom}}\right) + \left(F_{bottom} - DWOB \quad or \quad \left[F_{bottom} - DWOB\right]\times e^{-\mu|\theta|}\right) \quad \text{(no bending)} \tag{3}$$

$$F_{top} = \beta w \Delta L\left(\cos\alpha \quad or \quad \frac{\sin\alpha_{top} - \sin\alpha_{bottom}}{\alpha_{top} - \alpha_{bottom}}\right) - \mu \times \beta w \Delta L\left(\sin\alpha \quad or \quad \frac{\cos\alpha_{top} - \cos\alpha_{bottom}}{\alpha_{top} - \alpha_{bottom}}\right) + \left(F_{bottom} \quad or \quad F_{bottom} \times e^{-\mu|\theta|}\right) \quad \text{(bending)} \tag{4}$$

$$\begin{aligned} &\text{If RPM} > 14, \text{ no correction in WOB} \\ &\text{If RPM} < 14, \text{ WOB}_{\text{slide}} = \text{constant x } \Delta\text{p} \\ &\text{where, constant} = \frac{\left(\frac{\text{WOB}}{\Delta\text{p}}\right)_{i-2} + \left(\frac{\text{WOB}}{\Delta\text{p}}\right)_{i-3} + \left(\frac{\text{WOB}}{\Delta\text{p}}\right)_{i-4}}{3} \end{aligned} \tag{5}$$

Upon selecting a percentage value of SWOB as DWOB, ROP model developed for PDC (Hareland, G. et al., 2011) drill bits as illustrated with Eq. 6 was used. The ROP model of PDC drill bit considers a force balance between one cutter and formation to derive an analytical solution for entire drill bit face with multiple cutters. Such analytical solution was empirically calibrated (constants: K_1, a_1, b_1, c_1) with the laboratory data obtained with prototype drill bits tested on variety of formations (Warren and Armagost, 1988).

$$ROP = \left[\frac{K_1.WOB^{a_1}.RPM^{b_1}.\cos(SR)}{CCS^{c_1}.D_B.\tan(BR)}\right].W_f.h(x).b(x) \tag{6}$$

The empirical relation was further corrected for drill bit wear function (Eq. 7, 8) depending upon the formation abrasiveness, and wellbore cleaning efficiency based on bit hydraulics (Eq. 9 In addition to bit wear and hydraulic efficiency functions, the number of blades (N_b) of a PDC bit is considered to lower the drilling efficiency. This effect is applied using Eq. 11. The calculated ROP was iteratively matched to measured ROP and estimate CCS (Shirkavand, F. et al., 2009). The coefficients from hydraulic function (a_2, b_2, c_2) were determined from laboratory tests performed under simulated borehole conditions (Holster and Kipp, 1984). The CCS is correlated to UCS and YM using regression constants obtained from laboratory triaxial tests performed on Montney Formation core samples (Eq. 12, 13).

$$W_f = 1 - a_3\left(\frac{\Delta BG}{8}\right)^{b3} \tag{7}$$

$$\Delta BG = Ca\sum_{i=2}^{n} WOB_i.RPM_i.CCS_i.ABR_i \tag{8}$$

$$h(x) = a_2 \cdot \frac{(HSI \cdot \frac{JSA}{2 \cdot D_B})^{b_2}}{ROP^{c_2}} \tag{9}$$

$$HSI = \frac{HHP}{A_B} = \frac{[Q.P_B/1714]}{[(\pi/4)D_B{}^2]} \tag{10}$$

$$b(x) = \frac{RPM^{(1.02 - N_b x 0.02)}}{RPM^{0.92}} \tag{11}$$

$$UCS = \frac{CCS}{1 + a_s.Pc^{b_s}} \tag{12}$$

$$E = CCS.a_E.(1 + Pc)b_E \tag{13}$$

Results and Discussions

Wellbore friction was determined using time-based data and while drill string was lowered towards bottom with circulation and rotation. The selection of data points for depths were selected by four methods such off-bottom, 20 cm before off-bottom, 15 cm before off-bottom or suddent jump in stand-pipe pressure. The DWOB values computed by these four methods were compared and a constant percentage value of SWOB was selected as DWOB (83%) for subsequent ROP computations. Assumption of constant ratio of DWOB and SWOB in individual slanted or horizontal sections of the wellbore is consistent with real-time observations made by Belaskie et al. (1993). Figure 4 shows computed UCS and YM trends against measured depth in the horizontal section of the wellbore A. Clearly, uncertainties in drilling data points significantly affect the output trends. The average values of UCS and YM predicted with ROP models were found to be 99.57 MPa and 29.64 GPa respectively. Decreasing UCS profile in the later section of the wellbore (measured depth > 3500 m) indicates inaccurate drill bit wear evaluation on the rig. Figure 5 compares computed UCS trends for wellbore A with those obtained from sonic logs available on a part of the wellbore (measured depth: 2640-2790 m). Horsrud (2001) published correlations for predicting static mechanical properties such as UCS of shale using compressional velocity (V_p). UCS was computed with sonic log correlations by Horsrud (2001) (Eq. 14) and Onyia (1988) (Eq. 15). ROP models under predict UCS values than those derived from logs in this study and reported by Davey (2012) (UCS: 117-136 MPa) for the Montney Formation.

$$UCS_{MPa} = 0.77 \text{ x } V_{p_{km/s}}^{2.93} \tag{14}$$

$$UCS_{MPa} = \left[\frac{1}{5.15 \text{ x } 10^{-8} \left(\Delta t_{c\ \text{ft/s}} - 23.87 \right)^2} + 2 \right] \text{x } \frac{1}{145.077} \tag{15}$$

Figure 6 shows UCS and YM profiles generated on a horizontal section of wellbore B drilled in Montney Formation E lob with similar underbalanced drilling conditions and the identical PDC drill bit (MSF513M). The average values of UCS and YM were found to be 108.71 MPa and 32.37 GPa. Although results from Well A and B are consistent, Figure 6 confirms that fluctuations in drilling data points due to vibrations significantly affect the UCS and YM profiles. YM values estimated for the Montney Formation from drilling data are in agreement with those from laboratory measurements (range: 13.78-41.35 GPa) performed on Montney Formation cores (Hall and Jennings, 2011). Similarly, Keneti and Wong measured horizontal directional tensile and compressive elastic moduli of the Montney from Brazilian tests as 31 GPa and 40 GPa respectively.

The discrepancy in prediction of ROP models with those derived from logs could be related to uncertainties in drilling data. The depth-based data utilized in this prediction was not corrected to minimize erroneous data points due to mechanical events, vibrations and instrument sensitivity. The weight of hook, HL calibration, number of lines, true sheave efficiency and frictional losses in the sheave could significantly affect wellbore friction coefficient. Underbalanced drilling and gas influx can erroneously change effective mud weight in the wellbore and hence buoyancy forces. This study presents an approach to estimate actual (downhole) weight on bit based on the PDC bit cutting model and surface measurements. These results could be validated using high quality surface and downhole measurements which would allow separating actual rock strength variations from other potential causes of variable drilling loads (e.g. bit dulling, vibration, stabilizer hang-up). Subsurface core and log data from the early exploration and appraisal wells could be correlated to drilling data. These correlation could be further extrapolated across the field using only drilling data to build more robust areal distributions of the parameters such as confined compressive strength, unconfined compressive strength and Young's modulus which govern sweet-spotting of production well trajectories and stimulation designs.

Nomenclature

A_B	= bit face area
a_3,b_3	= empirical constants
a_1,b_1,c_1	= empirical constants
a_2,b_2,c_2	= empirical constants
ABR	= abrasiveness constant

BR	= PDC cutter back rake angle
b(x)	= function for the effect of number of blades
Ca	= bit wear coefficient
CCS	= confined compressive strength
D_B	= diameter of bit
DWOB	= downhole weight on bit
e	= individual sheave efficiency
F_{top}	= tension on the top of each drill string element
F_{bottom}	= tension on bottom of each drill string
h(x)	= hydraulic efficiency function
HHP	= hydraulic horsepower
HSI	= horsepower per square inch
JSA	= junk slot area
K_1	= empirical constant
N_b	= number of blades
n_{lines}	= number of lines between blocks
P_B	= bit pressure drop
Q	= pump flow rate
ROP	= rate of penetration
RPM	= surface/to-drive RPM
SR	= PDC cutter side rake angle
T_{dh}	= downhole torque
V_p	= compressional velocity
V_s	= shear velocity
w	= unit pipe weight
W_f	= bit wear function
WOB	= weight on bit
E	= Young's modulus
E_{dyn}	= dynamic Young's modulus
α	= inclination angle
β	= buoyancy factor
μ	= wellbore friction coefficient
ν	= Poisson's ratio
ΔBG	= cumulative bit wear
ΔL	= length of each drill string
Δp	= differential pressure
Δt_c	= compressional travel time

Acknowledgements

Authors would like to thank Shell International E & P Inc. and Shell Canada Ltd. for the permission to present this work and their invaluable assistance with drilling data. Authors express special thanks to Mohammad Moshirpour, Graduate student, University of Calgary. Authors also acknowledge John Dudley, Mark Dykstra, Alexei Savitski and Mauricio Farinas, Shell International E & P Inc. for their helpful suggestions.

References

Aadnoy, B.S. and Anderson, K. 2001. Design of Oil Wells using Analytical Friction Models. Journal of Petroleum Science and Engineering, 32, 1, 53-71.

Aadnoy, B., Fazaelizadeh, M. and Hareland, G. 2010. A 3D Analytical Model for Wellbore Friction. Journal of Canadian Petroleum Technology, 49, 10, 25-31, October.

Ajayi, B. et al. 2013. Stimulation Design for Unconventional Resources. Schlumberger Oilfield Review. 25, 2, 34-46.

Belaskie, J.P., Dunn, M.D. and Choo, D.K. 1993. Distinct Applications of MWD, Weight on Bit, and Torque. SPE Drilling and Completion, 111-117, June. Richardson, Texas: Society of Petroleum Engineers.

Burgess, T.M. and Lesso, W.G. Jr. 1985. Measuring the Wear of Milled Tooth Bits using MWD Torque and Weigh-on-bit. Paper SPE 13475 presented at the SPE/IADC Drilling Conference, New Orleans, Louisiana, 6-8 March.

Dangerfield, J.W. 1987. Analysis Improves Accuracy of Weight Indicator Reading. Oil and Gas Journal Technology, August.

Dashevskiy, D. et al. 2006. Dynamic Depth Correction to Reduce Depth Uncertainty and Improve MWD/LWD Log Quality. Paper SPE 103094 presented at the SPE Annual Technical Conference and Exhibition, San Antonio, Texas, USA, 24-27 September.

Davey, H. 2012. Geomechanical Characterization of the Montney Shale Northwest Alberta and Northeast British Columbia, Canada, M.S. Thesis, Department of Geology and Geological Engineering, Colorado School of Mines.
Edwards, D.E. et al. 2012. Triassic Strata of the Western Canada Sedimentary Basin, in Geological Atlas of the Western Canada Sedimentary Basin, G.D. Mossop and I. Shetsen (comp.), Canadian Society of Petroleum Geologists and Alberta Research Council, URL <http://www.ags.gov.ab.ca/publications/wcsb_atlas/atlas.html>, 11 September.
Eshkalak, M.O. et al. 2013. Synthetic, Geomechanical Logs for Marcellus Shale. Paper SPE 163690 presented at the 2013 SPE Digital Energy Conference and Exhibition, The Woodlands, Texas, USA, 5-7 March.
Falconer, I.G., Belaskie, J.P. and Variava, F. 1989. Applications of a Real Time Wellbore Friction Analysis. Paper SPE 18649 presented at the SPE/IADC Drilling Conference, New Orleans, Louisiana, 28 February – 3 Match.
Fazaelizadeh, M. et al. 2011. Real-time Wellbore Friction Analysis to Detect Onset of Drillstring Sticking during Extended Reach Well Drilling: Case Study. Paper SPE 143157 presented at the Brazil Offshore Conference and Exhibition, Macae, Brazil, 14-17 June.
Hall, C.D. and Jennings, D. 2011. Comparison of the Reservoir Properties of the Muskwa (Horn River Formation) with other North American Gas Shales.Paper presented at the Canadian Society of Petroleum Geologists Convention, Calgary, Canada, 9-13 May.
Hareland, G. and Hoberock, L.L. 1993. Use of Drilling Parameters to Predict In-situ Stress Bounds. Paper SPE 25727 presented at the SPE/IADC Drilling Conference, Amsterdam, Netherlands, 23-25 February.
Hareland, G. et al. 1996. Safe mud weight Window Predictor Instantaneous, Pre-planning and PostAnalysis Software. Paper SPE 26097 presented at the 4th Latin American/Caribean Petroleum Engineering Conference, Port-of-Spain, Trinidad, 23-26 April.
Hareland, G. et al. 2010. A New Drilling Rate Model for Tricone Bits and its Application to Predict Rock Compressive Strength. Paper ARMA 10-206 presented at the 44th US Rock Mechanics Symposium, Salt Lake City, Utah, USA, 27-30 June.
Hareland, G. and Nygaard, R. 2007. Calculating unconfined rock strength from drilling data. Proceedings of the 1st Canada-US Rock Mechanics Symposium, Vancouver, Canada, 27-31 May.
Holster, J.L. and Kipp, R.J. 1984. Effect of Bit Hydraulic Horsepower on the Drilling Rate of a Polycrystalline Diamond Compact Bit. Journal of Petroleum Technology, 2110-2118.
Horsrud, P. 2001. Estimating Mechanical Properties of Shale from Empirical Correlations. SPE Drilling and Completion, June.
Johancsik, C.A., Friesen, D.B. and Dawson, R. 1984. Torque and drag in directional wells – Prediction and Measurements. J. Pet Tech, 987-92.
Kuru, E. and Wojtanowsicz, A.K. 1988. A Method for Detecting In-situ PDC Bit Dull and Lithology Change. Paper SPE 17192 presented at the IADC/SPE Drilling Conference, Dallas, Texas, 28 February – 2 March.
Keneti, S.A.R. and Wong, R.C.K. 2011. Investigation of bimodularity in the Montney shale using the Brazilian test. Paper presented at the 45th US Rock Mechanical Symposium, San Francisco, California, USA, 26-29 June.
Lesage, M., Falconer, I.G. and Wick, C.J. 1988. Evaluating Drilling Practice in Deviated Wells with Torque and Weight Data. SPE Drilling Engineering, 248-252.
Luke, G.R. and Juvkam-Wold, H.C. 1993. Determination of True Hook Load and Line Tension under Dynamic Conditions. SPE Drilling and Completion, 259-264, December. Richardson, Texas: Soeciety of Petroleum Engineers.
Nieto, J., Bercha, R. and Chan, J. 2009. Shale Gas Petrophysics – Montney and Muskwa, Are they Barnett Look-Alikes? Paper SPWLA 84918 presented at the 50th Annual Logging Symposium, The Woodlands, Texas, USA, 21-24 June.
Onyia, E.C. 1988. Relationships Between Formation Strength, Drilling Strength, and Electric Log Properties. Paper SPE 18166 presented at the 63rd Annual Technical Conference and Exhibition, Houston, Texas, USA, 2-5 October.
Rampersad, P., Hareland, G. and Pairintra T. 1993. Drilling Optimization of an Oil or Gas Field. Paper SPE 26949 presented at the Eastern Regional Conference & Exhibition, Pittsburgh, Pennsylvania, 2-4 November.
Rassenfoss, S. 2011. Drilling Automation: A Catalyst for Change. Journal of Petroleum Technology. 28-35, September.
Reiber, F., Vos, B.E. and Eide, S.E. 1999. On-line Torque & Drag: A Real-Time Drilling Performance Optimization Tool. Paper SPE 52836 presented at the SPE/IADC Drilling Conference, Amsterdam, Netherlands, 9-11 March.
Sayers, C.M. 2010. The effect of anisotropy on the Young's moduli and Posson's ratio of shales. Presented at the 80th SEG Annual Meeting, Denver, Colorado, USA, 18-22 October.
Shirkavand, F., Hareland, G. and Aadnoy, B.S. 2009. Rock Mechanical Modeling for a Underbalanced Drilling Rate of Penetration Prediction. Paper ARMA 09-97 presented at the 43rd US Rock Mechanics Symposium, Asheville, North Carolina, USA, 28 June – 1 July.
Walsh, W. et al. 2006. Regional "Shale Gas" Potential of the Triassic Doig and Montney Formations, Northeastern British Columbia. Petroleum Geology Open File 2006-02, Oil and Gas Division, British Columbia, Canada.
Warren, T.M. 1984. Factors Affecting Torque for a Roller Cone Bit. J. Pet Tech, Vol. 36, 1500-1508. Richardson, Texas: Soeciety of Petroleum Engineers.
Warren, T.M. and Armagost, W.K. 1988. Laboratory Drilling Performance of PDC Bits. SPE Drilling Engineering, June.
Winters, W.J., Warren, T.M. and Onyia, E.C. 1987. Roller Bit Model with Rock Ductility and Cone Offset. Paper SPE 16696 presented at the 62nd Annual Technical Conference and Exhibition, Dallas, Texas, 27-30 September.
Unsworth, M.I., Burgess, T.M. and Kerbart, Y.J. 1990. How an Improved Depth Measurement and Smart Processing Can Help the Driller Improve Efficiency. Paper SPE 19965 presented at the IADC/SPE Drilling Conference, Houston, Texas, 27 February – 2 March.

Table 1: Depth resolved pore pressure, drilling fluid characteristics of Well A

Depth m	Pore Pressure kPa/m	Mud weight g/cc	Plastic viscosity mPa-s	Mud Type
2740	14.58	1.04	21	Oil-based
3504	14.58	1.03	19	Oil-based
4237	14.58	1.005	12	Oil-based
4490	14.58	1.355	30	Water-based

Table 2: Drill string specifications at total depth of Well A

Component Type	Joints	Length m	OD mm	ID mm	Specific mass Kg/m
Drill Pipe	192	1836.34	163	108	32
HWDP	39	362.91	164	77	70
Drill pipe	233	2250.35	163	71	32
Crossover	1	0.91	167	71	148
Flexible Drill Collar	1	8.79	155	73	148
Flexible Drill Collar	3	9.23	165	73	148
Pulser sub	1	2.93	149	59	148
MWD Tool	1	5.76	159	83	148
Crossover	1	0.65	157	78	148
Non-mag Pony Collar	1	2.99	166	73	148
Bent Housing	1	8.87	184	0	148
PDC	1	0.27	200	0	148
Total Length		4490			

Table 3: Design specifications of ReedHycalog MSF513M PDC drill bit

IADC Code	513
Diameter (mm)	200
Number of nozzles	7
Diameter of each nozzle (mm)	11.1
Number of cutters	33
Diameter of cutter (mm)	12.7
Back rake angle (deg.)	20
Side rake angle (deg.)	0
Cutter thicknerss (mm)	2
Junk slot area (mm^2)	76
Number of blades	5

Table 4: Typical gamma ray and abrasiveness constants for different rock types

Formation	Specific gravity	Abrasivess constant	Gamma ray
	-	-	API
Sand	2.6	1	10-30
Silts	2.67-2.7	0.85	50-70
Conglomite	2.4-2.9	0.71	10-140
Dolomite	2.7	0.65	<30
Limestone	2.7	0.57	<20
Shale	2.4-2.8	0.11	80-300
Coal bituminous	1.35	0.1	20

Era	Period	Formation Top	MD (m)
Mesozoic	Lower Cretaceous	Paddy	766.14
		Cadotte	793.22
		Harmon	835.89
		Notikewin	891.9
		Falher	952.65
		Wilrich	1171.42
		Bluesky	1237.51
		Gething	1267.49
		Cadomin	1420.55
	Jurassic	Nikanassin	1445.87
		Fernie	1616.11
		Nordegg	1721.52
	Triassic	Baldonnel	1751.1
		Pardonet	1740.35
		Charlie Lake Fm	1794.58
		Artex	2151.19
		Halfway	2162
		Doig	2211
		Phosphate (Upper)	2332
		Phosphate (Middle)	2346.38
		Phosphate (Lower)	2377.6
		Montney	2392.19
		MNTN E Lobe	2396.32

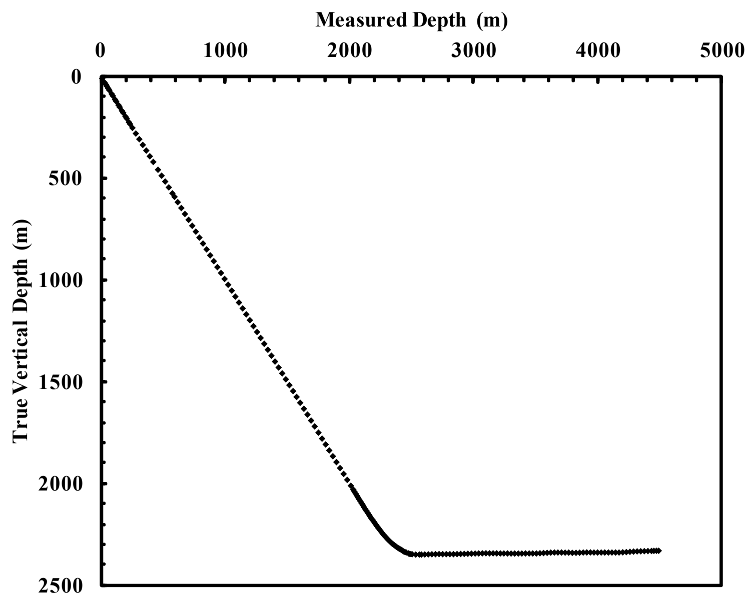

Figure 1: Formation intervals and plot of true vertical depth against measured depth for the horizontal well (Well A) completed in Montney Formation E lobe.

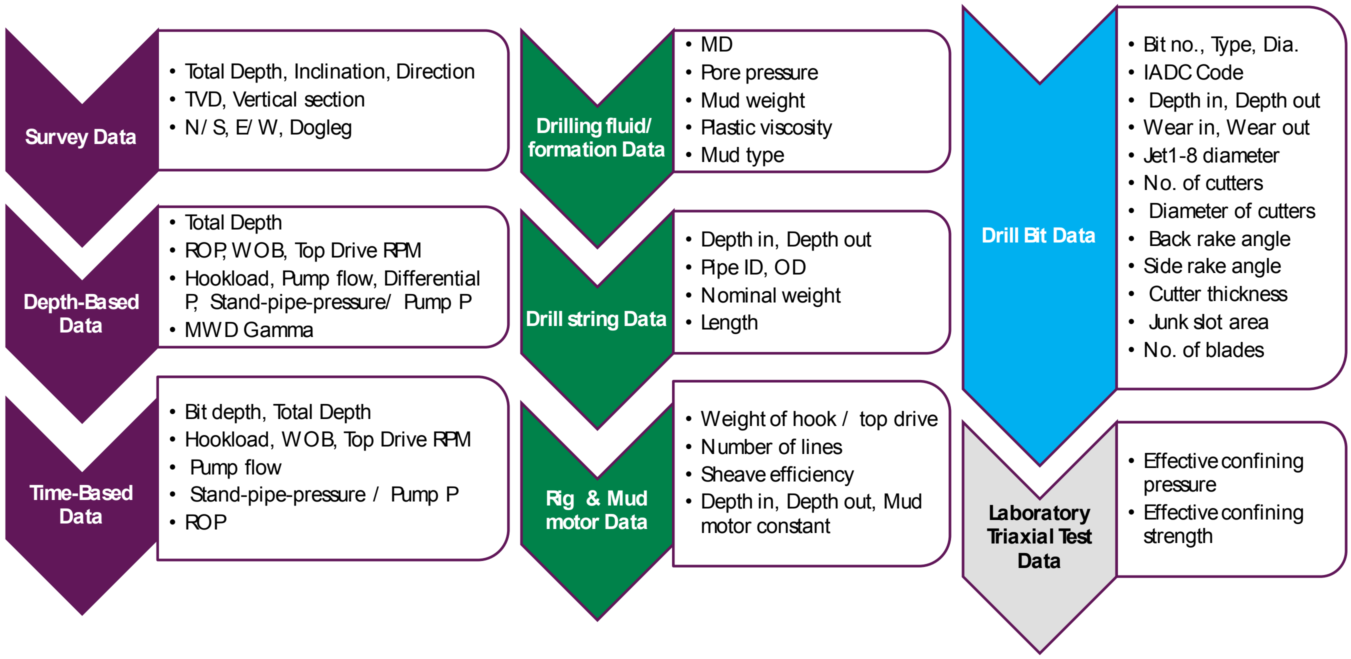

Figure 2: Summary of inputs used in DWOB-DROCK software calculations.

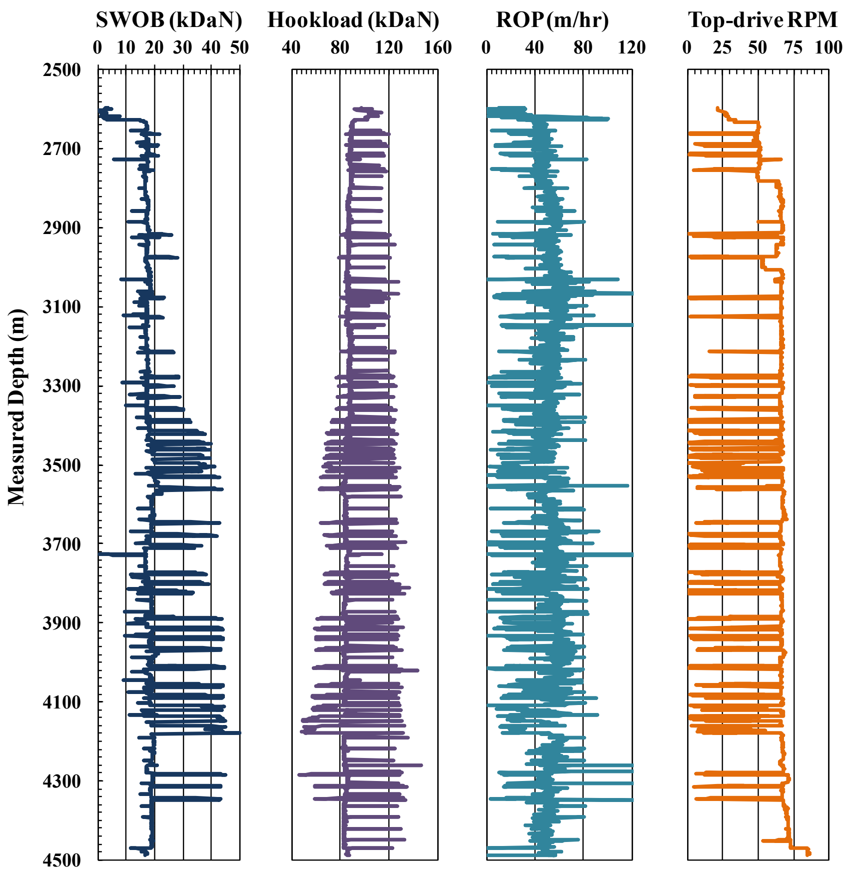

Figure 3: SWOB, HL, ROP and top-drive RPM from the depth-based file of Well A.

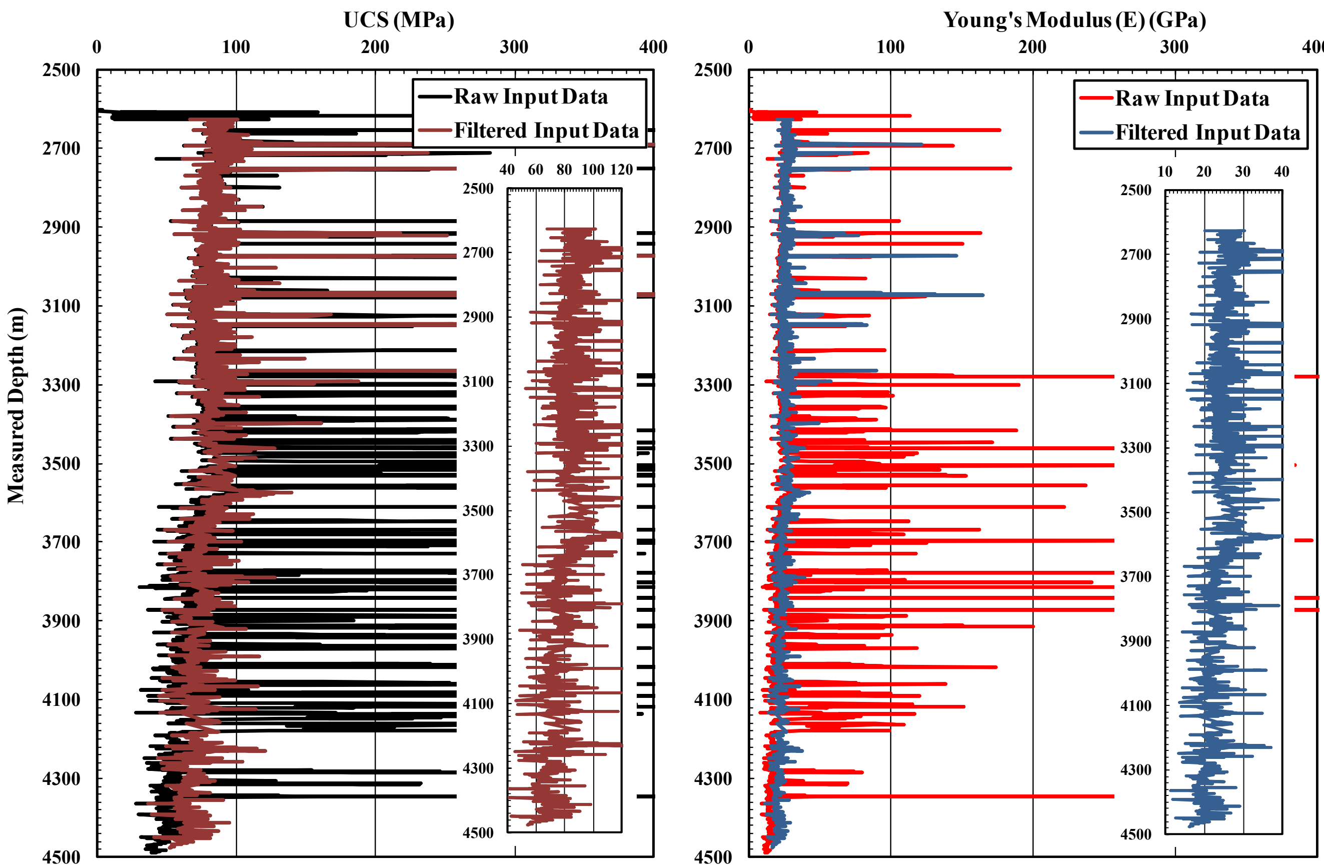

Figure 4: UCS (left) and YM (right) computed for Well A with raw and filtered drilling data as input.

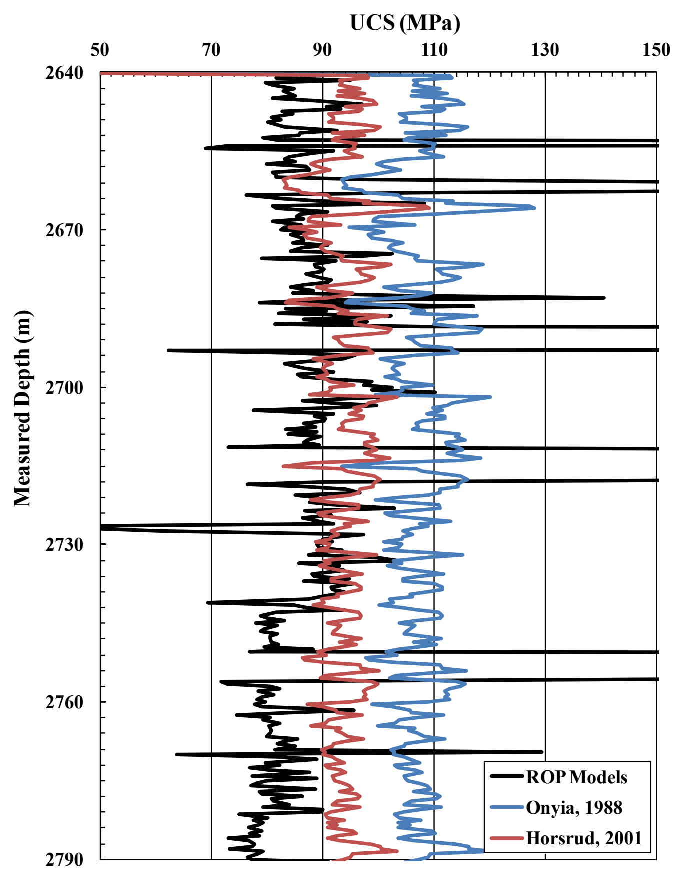

Figure 5: Comparison of UCS profile obtained from ROP models for Well A with those obtained from sonic logs.

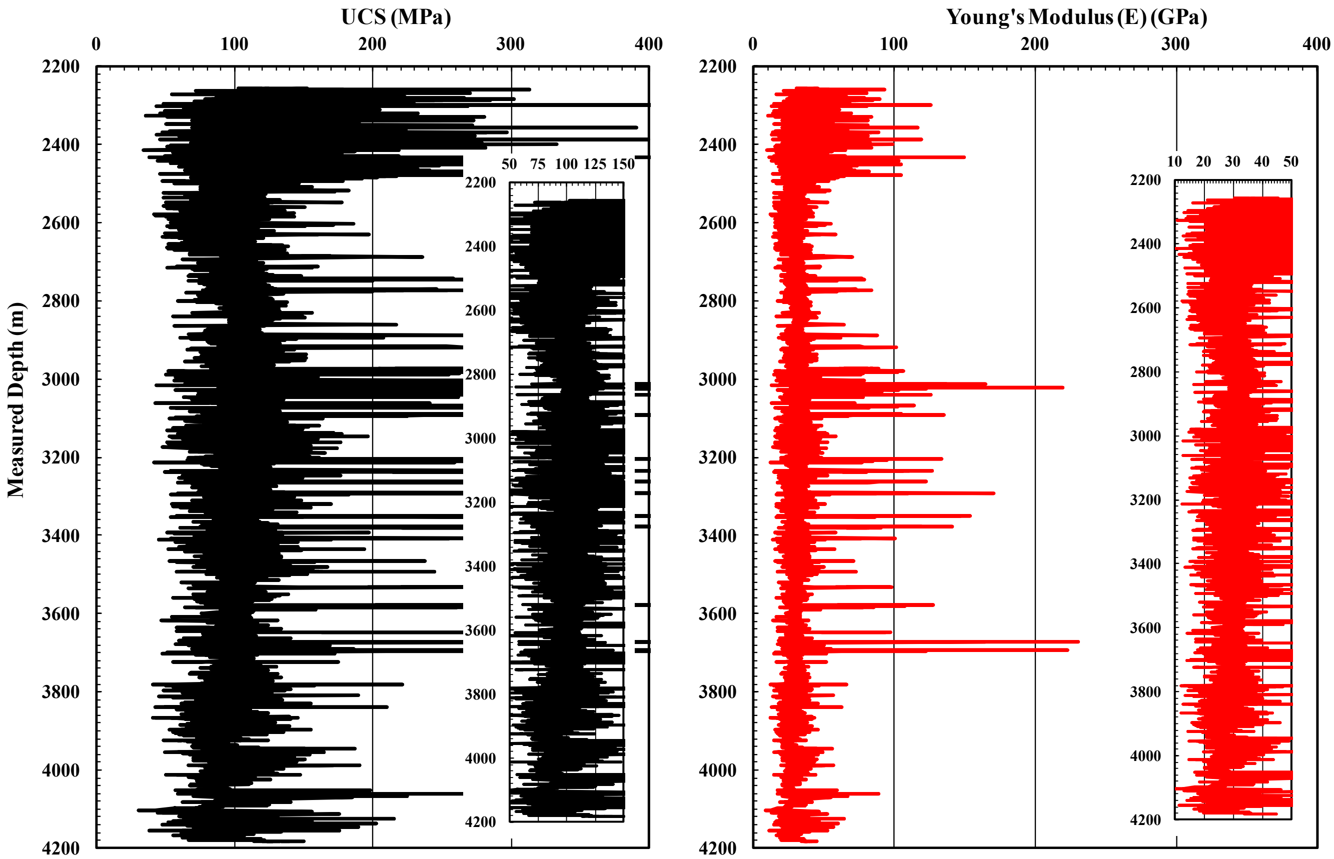

Figure 6: UCS (left) and YM (right) computed for Well B with raw drilling data as input.